specific geometric places. Secondly, the tools must be constantly in contact with the surface, so as to manufacture it smoothly and accurately. Thirdly, the radius of the tool surface must be calculated so that the curves of the blade surface are correctly manufactured. Finally, the forth condition is the position of the cutting tool at the surface in order to appropriately manufacture the stock and prevent from any fault positioning.

For the blade manufacturing, the CAD file was imported in CAM software Nx for further analysis. With the aid of this software, the strategy of the blades manufacturing was decided and programmed with respect to the quality of the final product, addressed through a parameter of great importance, namely surface roughness and the required machining time. The manufacturing process took place in a CNC machining center Milltronics VM20 with four axes indexed. The tools used were a flat end mill of diameter equal to 25.4 mm and two ball end mills tool with 12 mm and 8 mm of diameter. The workpiece material employed was Prolon MS (Castnylon + Molybdenum). Taking into account the geometry of the blade, the strategy that has to be followed during roughing and finishing procedure was decided.

Initially, due to the high cost of this material, the geometry of the prolon billet was optimized to reduce wastes. For this purpose, a plate allowing two blades machining was taken as reference. For this reason, the first step was to separate the billet machining of each blade, as shown in Fig. 2a. This operation was carried out by designing a sketch to define the path of the cutter to cut the material. From this line, a profile of operation was performed, as presented in Fig. 2b.

a)

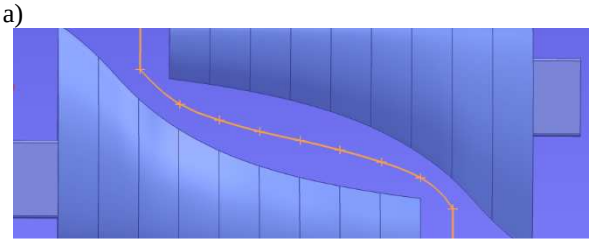

b)

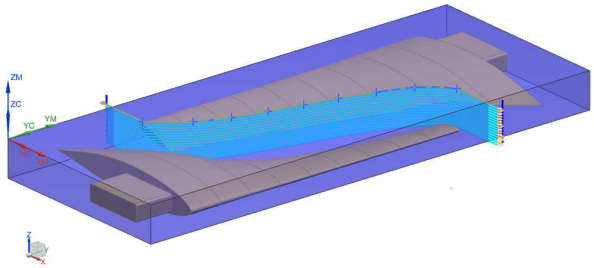

Fig. 2. Processes for cutting the prolon billet. a) Assemble and sketch, b) Simulation paths for cutting.

Due to size limitations of the bench, the process was conducted with the fixed billet at the table of the machining center without the use of the fourth axis. Machining on each side, the part was manually rotated; where, to ensure zero workpiece during rotation, they were fixed to the table three (3) records in steel, before the machining, as shown in Fig. 3.

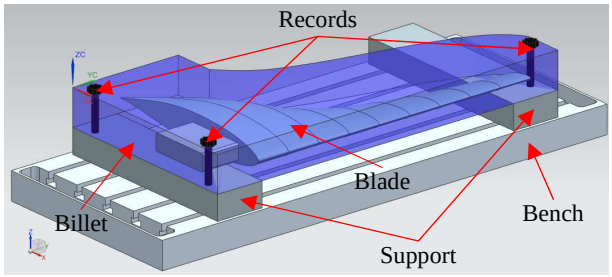

Fig. 3. Assembly of the turbine manufacturing process.

Two roughing steps and one finishing step were selected. In the first roughing step, higher depth or cut was used in order to reduce the machining time, while in the second roughing step, finer cutting conditions were used to prepare the material for the finishing operation. The latter gave to the blade the high quality characteristics that it requires to be operational. For roughing and finishing, three possible tool trajectories could be selected, namely cyclic, spiral or plain straight lines. The analysis showed that spiral movements of the tool gave better results at acceptable time, both for roughing and finishing operations.

Furthermore, in relation to the workpiece material machining conditions; i.e., cutting speed, feed rate and depth of cut, were chosen after many combinations performed with the CAM tools, so as to have a smooth and clear final surface. The cutting parameters were calculated based on the equations (1) (2) (3) and are represented in the Table I.

$$n = \frac{v_c * 1000}{\pi * D_{cap}} \quad (1)$$

$$D_{\mathrm{cap}} = \sqrt{\mathrm{Dc}^2 - (\mathrm{Dc} - 2.\,\mathrm{a_p})^2} \quad (2)$$

$$v_f = n * Z_n * f_z \quad (3)$$

where, v_c is the cutting speed (m/min), D_c is the diameter of the tool (mm), f_z is the feed per tooth (mm/tooth), n is the spindle speed (rpm), Z_n is the number of effective teeth, $D_{cap,}$ is the diameter at the depth of cut (mm), $a_{p:}$ is the depth of cut (mm) and v_f is the feed speed (mm/min). Both f_z and v_c are data provided by the tool manufacturer. The machining steps are presented in Fig. 4.

Table I. Machining cutting parameters of the blade.

Operation	Parameters	Value
First roughing	Cutting speed (mm /min)	2300
	Rotation speed (rpm)	4200
	Depth of cut (mm)	0.3
	Oversize (mm)	1.0
	Flat end mill (mm)	25.4
Second roughing	Cutting speed (mm /min)	1820
	Rotation speed (rpm)	6540
	Depth of cut (mm)	0.15
	Oversize (mm)	0.2
	Ball end mill (mm)	12
Finishing	Cutting speed (mm / min)	2053
	Rotation speed (rpm)	7000
	Depth of cut (mm)	0
	Oversize (mm)	0
	Ball end mill (mm)	8

a)

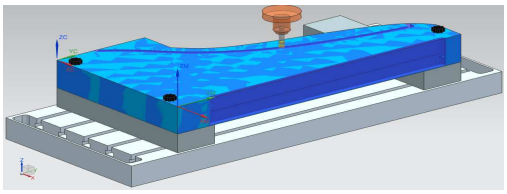

b)

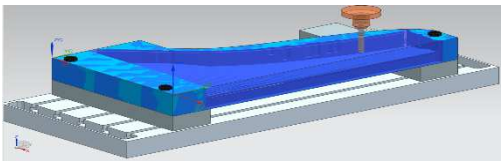

c)

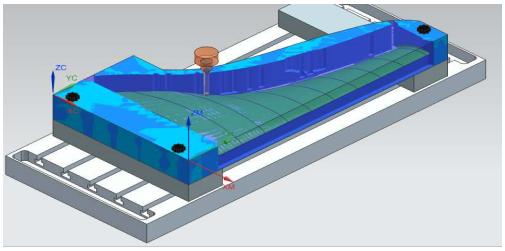

d)

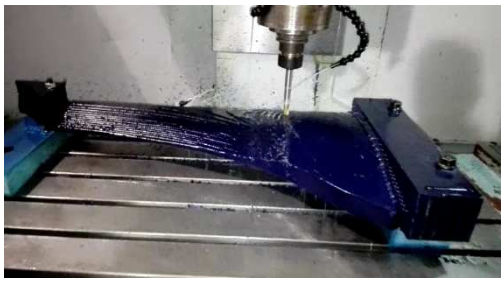

Fig. 4. CAM software snapshots and real machining process. (a) roughing of the upper surface and blades with flat end tool (b) roughing of the blades (c) finishing of the blade with ball end tool and (d) finishing of the blades with ball end tool (real machining process).

Once the process was completed on the surface 1, the prolon billet was turned 180° for the machining of surface 2, for which the same strategy defined above was used. Finally, a profiling operation was performed to reach the final shape of the blade (Fig. 5).

Fig. 5. Blade of the hydrokinetic turbine manufactured by CNC

In general, the complex geometry of the blade, although is a challenge for the machining process, modern software and cutting and machine tools can overcome any problem imposed and realize the final workpiece geometry in relatively low machining times and with high quality characteristics.

Once the blades and the hub were made, the turbine was mounted on a frame with adjustable height, which was attached to a floating platform designed especially for this purpose. This floating platform consisted of a raft formed by several modular parts (Fig. 6) that provide unlimited configurations of the surface of floating; i.e., the floating cubes can be assembled to create the desired shape and size. The blocks were held together tightly and firmly with special connecting pins. All parts were lightweight and easy to handle. They were made or high density polyethylene resin. Candock cubes are remarkably resistant to impact, climate change and the adverse effects of water. The floating capacity of the surface formed was 680 kg, although the turbine and supporting structure alone weighed approximately 250 kg. In general, the floating raft provided a platform for operation and maintenance activities. The hydrostatic stability of the platform in static and towing conditions was studied for different positions of the turbine with respect to the water level.

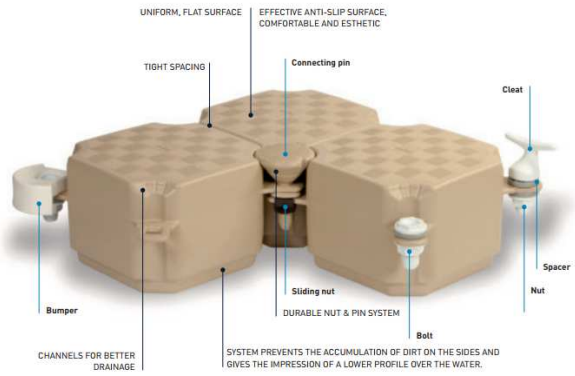

Fig. 6. Modular floating system. Candock (www.candock.com)

4. Experimental evaluation of the hydrokinetic turbine

It is well known that the best performance and the highest power production of the hydrokinetic turbine is made by a smooth linear flow of water at high velocity. The flow characteristic of a river stream has a stochastic variation, both seasonal and daily. Additionally, the water velocity varies from one potential site to the other depending on the cross-sectional area; therefore, the location of the turbine in the water current turbine must be very well considered.

The placement of the hydrokinetic turbine, in relation to the river cross-section, is a very significant component for two basic reasons. First of all, the energy flux in the surface of a stream is higher than that of the stream on the bottom. In addition, this quantity takes diverse values depending on the distance from the river bank [3]-[6]. The water current in a river may vary depending on the bottom. Therefore, the water velocity has a localized and site-specific profile, and the location of the rotor dictates the amount of energy that can be produced. Secondly, in a river there are competing users of the water stream,

such as boats, fishing vessels, bridges, etc.; and these might reduce the effective usable area for a turbine installation [3], [5], [6]. There could also be varying types of suspended particles and materials like fish, rock, etc. in the river. In general, properly placing a hydrokinetic turbine requires an understanding of what influences the kinetic energy or velocity of the water at any point in the river.

The hydrokinetic system developed (Fig. 1) consists of a hydrokinetic turbine, gear, generator, power conversion interface and battery/grid. When the turbine is merged into the water, the flowing current turns the turbine, and the coupled generator rotor will spin along with the turbine shaft. If an induction machine is used as the generator, a gearbox is required between the generator and the turbine to produce the corresponding frequency during the lower water speed; nevertheless, the permanent magnet synchronous generator can connect to the hydrokinetic turbine directly. A gearbox system can provide machine noise, losses and increase the cost of the system for frequent maintenance. In addition, the gearbox also makes the hydrokinetic system more complicated with less reliability [3]-[6].

The output power is controlled and converted by power conversion interface. For a grid-connected system, an inverter connects to the DC bus to convert the DC power to AC power and exporting such as power to the power grid. For a stand-alone system, a load and a battery pack are attached to the DC bus. The resistive load is used to dissipate the extra power produced by the system when the battery is fully charge.

The performance of the hydrokinetic turbine designed was mainly characterized through the power coefficient (C_P) measurement. This Coefficient can be defined as ratio of output mechanical power of turbine (P) to the inlet kinetic energy of water per unit time or the total amount of the hydrokinetic energy that can be converted into mechanical energy by turbine. C_P can be calculated according to Eq. (4).

$$C_P = \frac{P}{0.5\rho\pi R^2 V^3} \qquad (4)$$

where $\boldsymbol{\rho}$ is the water density (997 kg/m^3), R is the turbine radius (0.79 m) and V is the flow velocity. The power coefficient refers to a measure of the blade or hydrofoil efficiency. It includes the hydrofoil shape and the hydrodynamic force of lift and drag. The electrical power output can be calculated according to Eq. (5) [10, 11, 12].

$$P_e = \eta C_P 0.5\rho\pi R^2 V^3 \qquad (5)$$

The term η, is a measurement of the efficiency of the gearbox, drive train, the electrical inverter and the generator. This variable takes into account all the friction, slippage and heat losses associated with the internal mechanical and electrical components. Values of η may greatly differ among the different turbine models. The range of values of η are presented in the literature, highlighting the study conducted by Hangerman et al. 2006, which states a range of efficiencies between 95% to 98% [13]. However, for the design of the blade, a reasonable and conservative value of η around 70% was used [2, 10, 11, 12].

The product of the variables C_p and η is the overall equipment efficiency. For the measurement of this parameter, the turbine was paced in operation in the Sinú River, located in the state of Córdoba (Colombia). Initially, the turbine was transported to the site in the back of a pick-up truck (Fig. 7). A potential turbine site being accessible by road is a major advantage as it makes installation and maintenance a quick and easy process.

Fig. 7. Transport of the hydrokinetic turbine to the Sinú River.

Once the turbine was assembled on the river bank, it was towed to the final site of installation. The turbine was anchored to the river bottom using galvanized steel bars of 8 m in length (Fig. 8). Installation was completed in less than two hours, demonstrating the efficiency of the hydrokinetic installations. Smaller turbines, especially the portable turbines, should present fewer complications and result in even simpler installations.

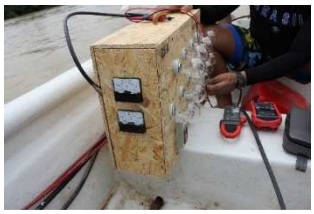

Fig. 8. Installation of the hydrokinetic turbine.

Once the turbine was installed, it was submerged in the stream of the Sinú River. For the installation of the submerged turbine, having enough width and depth of about 2 m is an important factor. The installation site had a depth of approximately 5 m. The turbine was installed in a region with a very constant river flow.

Once paced in operation, the power generated from the hydrokinetic turbine was transmitted to the power control center, which also contained a resistance bank (9 bulbs of 100 W each), and it was used as a load. Furthermore, a clamp current meter and a voltmeter were used to measure the power. The measurements did not provide significant results concerning the power generation due to the water velocity at the entrance of the turbine was only approximately 0.625 m/s; thus, the maximum power available in the water that can be transformed into electrical energy was 238.621 W. The turbine produced a maximum electrical power output of 127.89 W; therefore, the overall equipment efficiency was 0.5359.

Assuming that power coefficient of the turbine is the maximum theoretical power coefficient (C_{pmax}=16/27), the efficiency η of the turbine is 90.43%. On the other hand, if the power coefficient is equal to the value assumed for the design (0.4382), η is 73.94%. The turbine exhibited self-rotating characteristics whenever the water current speed crossed the cut-in speed of 0.625 m/s. Finally, the turbine was retrieved from the Sinú River after successful completion of the trial.

5. Conclusion

The hydrokinetic turbine designed to produce an electrical power output of 1 kW at approximately 1.5 m/s water current speed can provide a complete renewable energy solution for the remote communities in the developing countries. The developed technology is standardized and easily scalable. Qualified as a "green" technology, this product is positioned as the best alternative for decentralized electrification along rivers.

The turbine was rigorously tested in the Sinú River, located in Córdoba (Colombia). At this location, the turbine was suspended below the water surface from a special designed floating platform. The turbine was found to be self-starting at speeds near to 0.625 m/s. The overall equipment efficiency was estimated to be 0.5359.

During the designing process of the blade, it is essential to choose a simplified method construction, allowing making the blade locally in rural communities or near them for reducing turbine total costs. Technically, the turbine can be fabricated by a wide range of methods, ranging from hand carving up to CNC machine.

Acknowledgement

The authors gratefully acknowledge the financial support from Universidad de Antioquia and the Colombian Institute of Science and Technology (COLCIENCIAS).

References

[1] Rubén D. Montoya Ramírez, Felipe Isaza Cuervo, César Antonio Monsalve Rico, "Technical and financial evaluation of hydrokinetic power in the discharge channels of large hydropower plants in Colombia: A case study", Renewable Energy, Volume 99, pp 136-147, 2016.

[2] M. Anyi and B. Kirke, "Evaluation of small axial of hydrokinetic turbines for remote communities", Energy for Sustainable Development, vol .14, no 2, pp. 110-116, 2010.

[3] H.J. Vermaak, K. Kusakana, and S.P. Koko, "Status of micro-hydrokinetic river technology in rural applications: A review of literature", Renewable and Sustainable Energy Reviews, vol. 29, pp. 625-633, 2014.

[4] M.S. Gney and K. Kaygusuz, "Hydrokinetic energy conversion systems: A technology status review", Renewable and Sustainable Energy Reviews, vol. 14, no 9, pp. 2996-3004, 2010.

[5] Nicholas D. Laws, Brenden P. Epps, Hydrokinetic energy conversion: Technology, research, and outlook, Renewable and Sustainable Energy Reviews, Volume 57, Pages 1245-1259, 2016.

[6]. M. Anyi and B. Kirke, "Hydrokinetic turbine blades: Design and local construction techniques for remote communities", Energy for Sustainable Development, vol. 15, no 3, pp. 223-230, 2011.

[7] Martin Anyi, Brian Kirke, Tests on a non-clogging hydrokinetic turbine, Energy for Sustainable Development, Volume 25, pp 50-55, 2015.

[[8] A.H. Muñoz, L.E. Chiang, and E.A. De la Jara, "A design tool and fabrication guidelines for small low cost horizontal axis hydrokinetic turbines", Energy for Sustainable Development, vol. 22, pp. 21-33, 2014. Wind Power Special Issue.

[9] James F. Manwell, Jon G. McGowan, and Anthony L. Rogers, "Wind Energy Explained: Theory, Design and Application", Wiley, pp. 23-155, 2009.

[10] E. Chica, F. Pérez, A. Rubio-Clemente and S. Agudelo, "Design of a hydrokinetic turbine", WIT Transactions on Ecology and The Environment, Wessex Institute of Technology, 195 137-148, 2015.

[11] E. Chica, F. Pérez and A. Rubio-Clemente, "Rotor structural design of a hydrokinetic turbine", International Journal of Applied Engineering Research, 11 (4), 2890-2897, 2016.

[12] Chica E and Rubio-Clemente A, "Design of zero head turbines for power generation", Chapter of book in Renewable Hydropower Technologies, ISBN 978-953-51-3382-7. Print ISBN, 2017.

[13] Hagerman G, Polagye B, Bedard R, Previsic B. "Methodology for estimating tidal current energy resources and power production by tidal in-stream energy conversion (TISEC) devices". Rep. EPRI-TP-001 NA Rev 2, Electr. Power Res. Inst. Palo Alto, CA. 2006.